

## 2. ACCELERATOR AUGMENTATION PROGRAMME

### 2.1 LINAC

P.N.Prakash, S.Ghosh, R.Mehta, A.Sarkar, G.K.Chaudhari, S.S.K.Sonti,  
D.S.Mathuria, K.K.Mistri, A.Rai, J.Zacharias, J.Antony, R.K. Bhowmik and A.Roy

The previous year saw the commissioning and operation of all the facilities connected to the indigenous fabrication of superconducting resonator project. Fabrication of the first indigenous niobium resonator is nearing completion. The first linac module is also being readied for beam tests. A new resonator testing facility has become fully operational. The high energy sweeper has been installed and tested in the beam line. Details of all the major developments are presented below.

#### 2.1.1 Superconducting Resonator Fabrication Facility - SuRFF

##### (i) Surface Preparation Laboratory (SPL)

The surface preparation laboratory is now fully operational. Figure 1 shows the fume hood and the acid circulating pump. Four doubled walled teflon tubes with valves are laid to transfer and recirculate the acid. The acid pump was initially tested for leaks with water for nearly 36 hours. Adequate safety precautions have been taken in designing the system such that the acid is always contained in doubly shielded containers. Other utilities like ultrasonic cleaner, closed loop water chiller unit, 0-20V, 1000 Amp power



**Fig. 1 : Fumehood**



**Fig. 2 : Surface Preparation Lab**

supply have been integrated and tested in SPL.

A niobium strip was electropolished for 100 cycles to calibrate the material removal rate. Several resonators and parts have been successfully electropolished since. Figure 2 shows another view of SPL with the stainless steel sink, safety shower, eye wash, acid refrigerator and water chiller in place. The high pressure rinsing system (80 bar) has been fully commissioned inside the class 100 clean room (located in SPL).

**(ii) High Vacuum Furnace**

The high vacuum furnace has already been commissioned. A niobium getter box of size  $\varnothing 600 \text{ mm} \times 1000 \text{ mm}$  is being fabricated for the heat treatment of the resonators.

**(iii) Electron Beam Welding Machine - EBW**

The electron beam welding machine (Figure 3) was commissioned in January '2002. Machine calibrations were performed prior to developing welding parameters for niobium. In the EBW machine the table can travel along the X axis and the gun moves in the Y direction. Movement in the Z axis is controlled by adjusting the current in the focus coil. In order to develop parameters that were reproducible, the focus coil current was calibrated. For this several 'bead on plate' samples were performed at different gun to work distance. The samples were cut, mechanically polished and chemically etched to determine the maximum penetration depth. In all, more than two dozen samples, each having more than a dozen weld passes, were made. Similarly the vibration and deflection coil was calibrated at different gun to work distances to determine the beam oscillation size and deflection angle.



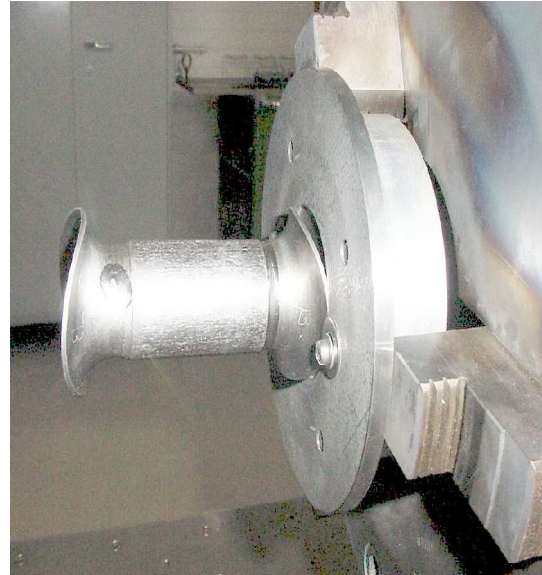
**Fig. 3 : Electron Beam Welding Machine at Nuclear Science Centre**

Following the machine calibrations niobium welding parameters were developed for the NSC-QWR. Initially bead on plate samples were made for the two thickness of materials and later resonator sample parts were welded to fine tune the parameter. The criteria for welding were full penetration with minimum undercut and underfill, no porosity, smooth face and root. Using these criteria welding parameters were developed in the conductance mode. In addition, parameters were also developed in the key hole process. Some of the welds were thermally shocked several times from room temperature to liquid nitrogen and leak tested at  $< 2 \times 10^{-9}$  mbar lt/s.

### **2.1.2 Indigenous Fabrication of Niobium Resonator**

During the resonator production at Argonne National Laboratory several additional resonator parts were fabricated. Also some parts were fabricated a few years back during a separate project to fabricate niobium resonators indigenously. We felt it was prudent to construct the first resonator using all the parts available from these two projects and fabricate those parts which were not available, in the NSC workshop. This way we could get hands on experience in handling, machining, fitting and most importantly the electron beam welding of niobium resonator parts. Figure 4 shows the EBW setup of ports to the outer niobium housing. Figure 5 shows fixing up of the blow through in the drift tube beam port assembly. Figure 6 shows the setup for welding the top flange to the central conductor assembly of the quarter wave resonator. Figure 7 shows the central con-

ductor assembly and the outer housing ready for the closure weld. At the time of writing this report the bare niobium portion of the resonator was ready. After electropolishing and heat treatment the resonator would be jacketed in the outer stainless steel vessel and



cold tested.

**Fig. 4 : Weld setup for Nb Housing**

**Fig. 5 : Fixing of blow through in the Drift Tube Beam Port assembly**



**Fig. 6 : Top Flange to Central Conductor Welding setup**

**Fig. 7 : Nb Outer Housing and Central Conductor Assemblies**

In addition to the first resonator, two more resonators are being fabricated using all parts made indigenously. After the successful completion of this project, fabrication of the remaining resonators for the linac would be taken up.

### 2.1.3 Installation and Testing of the High Energy Sweeper

In the new pulsing system of NSC the multiharmonic buncher (MHB) and the phase detector had been installed and operated successfully. Bunched beam of FWHM 1.5 ns with efficiency > 50% will be delivered to the booster linac and other experimental beam lines. To remove the dark current between two successive peaks of the bunched beam a high-energy sweeper (HES) was designed, fabricated and installed in the beam line. The resonance frequency of the HES is 6.06 MHz and the quality factor Q achieved is 1300. Figure 8 shows the HES with its tank circuit installed in the post analyzer section of the Pelletron beam line. Figure 9 shows the deflector plates of the sweeper. The sweeper slit, which allows the bunched peak to pass through and block the dark current, was installed about three meters down stream immediately after the energy slit of the Pelletron. Special precautions were taken to align the sweeper and maintain the parallelism of the deflector plates and their perpendicularity to the beam axis.

In the offline high power test of the sweeper a voltage of about 31 kV peak to peak was achieved across the deflector plates at an input power of 350 Watts. In the on-line performance test,  $^{28}\text{Si}^{+8}$  bunched beam of energy 113 MeV was injected into HES and transported up to the diagnostic box installed at the entrance of the first linac cryostat. Surface barrier detector, mounted inside the diagnostic box, was used to measure the energy and time width of the beam. With the HES off, the peak to total current ratio was measured to be 60%, i.e. 60% of the DC beam was under the bunched peak and the rest 40% was spread between two successive peaks. When the HES was turned on during a short run of about ten minutes, the best value of peak to total current ratio was measured to be 97%, as shown in Fig. 10. Long term stability of the sweeper could not be tested due to malfunction in the phase lock loop of the sweeper controller. Modifications in the same are presently being done for checking the long term stability of the entire system.

**Fig. 8 : HES with the tank circuit**

**Fig. 9 : Sweeper deflector plates**

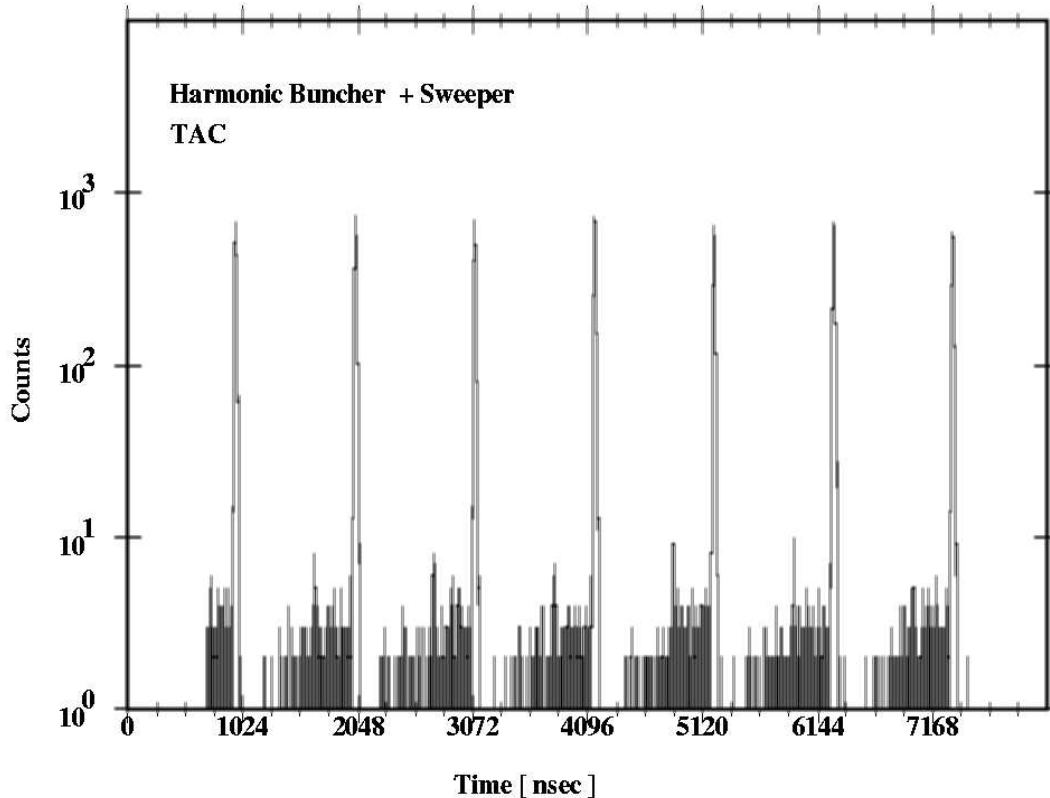


**Fig. 10 : TAC Spectrum shows a peak to total current ratio of about 97%.  
Data on Y axis is plotted on logarithmic scale**

#### **2.1.4 Status of Simple Test Cryostat facility**

To conduct offline performance tests of superconducting resonators a Simple Test Cryostat (STC) was fabricated and tested. Substantial amount of work has been done this year to fabricate and install various components for resonator testing. This includes the RF drive coupler and pickup, RF power line, drive coupler movement mechanism, slow tuner gas line connection, arrangement for pre-cool and bake out etc. Several electronic controllers, e.g. drive coupler stepper motor, vacuum interlock controller, temperature controller have been made. The RF rack is also being modified by adding superior quality components, in particular, bi-directional coupler and linear attenuators. Lead and mu-metal sheets were wrapped around the cryostat for radiation protection and to prevent the resonator from earth's magnetic field. To achieve easy loading and operation of the resonator in STC, two thirds of the cryostat vessel was buried inside a pit dug up in the beam hall. This was a cumbersome affair since the beam hall is situated on large rocks and boulders and the pit had to be dug up mostly by hand. In addition the entire STC facility is being given a permanent shape by laying water, compressed air, dry nitrogen gas lines, and electrical outlets. The STC facility is fully operational and resonators are being tested routinely although it may take a few more months to accord it the permanent shape. Figure 11 shows a resonator with all its accessories ready for loading in STC.



**Fig. 11 : Simple Test Cryostat top insert with a resonator**

### **2.1.5 Linac Beam Line**

The beam line up to the entrance of the first linac module has been installed and leak tested. The first linac module has been aligned and checked with beam. A Complete three dimension layout of the linac beam line from existing analyzer magnet to beam hall-II switching magnet has been prepared, which makes it extremely useful for laying out various utilities e.g. electric, pneumatic, water lines etc. All components of the beam line are stored in a library and can be extracted for future beam line designs. Two new high vacuum diagnostic chambers with target ladder and indigenously developed Faraday cup have been installed in the beam line. The diagnostic chamber also has provision for mounting surface barrier detector, PMT, and cooling arrangement for the detectors. Twelve new drive couplers have been fabricated. These drives have different linear travel and loop size for optimum design for installation in the linac cryostat.

Three phase detectors were installed in the linac beam line. The first phase detector will be used to monitor the phase of the beam at the entrance of the first linac module. The remaining two phase detectors will be used to measure the beam energy at the exit of the third linac module. The phase detectors are made out of SS-304 and copper tube. Two out of three phase detectors have been silver plated. A quality factor of 2600 was meas-

ured for the plated cavities, whereas the quality factor of the unplated cavity was measured to be about 1800.

### **2.1.6 Linac Cryostat**

The first linac module is being prepared for beam tests with resonators. RF power cable and pickup cables from the top of the cryostat to the resonators are routed through liquid nitrogen vessel inside the cryostat. Special feedthroughs, compatible at LN<sub>2</sub> temperature, have been used to separate the liquid nitrogen vessel from the vacuum space inside the cryostat. All the drive probes, pickup probes with their adapter flanges have been installed. The slow tuner lines with feedthrough flanges have been installed. For moving the drive couplers, rotary motion feedthroughs have been installed and coupled to the drive probes using shafts, universal couplings and rack and pinion. A cold test was conducted at liquid nitrogen temperature to perform RF checks, which were successful. All the mechanical assemblies also worked satisfactorily.

### **2.1.7 Development of High Energy Sweeper Controller**

A controller for driving the High Energy Sweeper has been fabricated and tested in the Laboratory. This controller takes 6.06250 MHz RF input from the clock distribution system and generates the drive signal for the sweeper. It has the provision for changing the amplitude and phase of the drive signal. Once the right amplitude and phase are set they need to be locked. So both phase and amplitude locking arrangements are done in the module. The module has been tested thoroughly in the laboratory and found to work satisfactorily. Long duration stability tests have been conducted running the module along with the power amplifier and both amplitude and phase were found to be stable under locked conditions. The phase locking could correct the phase with a stability of  $\pm 100$  ps.

### **2.1.8 Optimization of Multi-harmonic Buncher and Testing of High Energy Sweeper with DC and Bunched Beams**

Initially the dc beam produced by the Pelletron was used to check the different parameters of the High Energy Sweeper. Then the Multi-harmonic buncher was optimized in a systematic manner. First of all only 12MHz RF was put on to bunch the beam. Then the higher harmonics viz. 24MHz and 36MHz were added one by one in proper phase and amplitude to optimize the saw-tooth voltage across the buncher grids. With proper fine tuning a bunched beam of  $^{28}\text{Si}$  with an efficiency  $\sim 60\%$  and FWHM 1.5 ns was obtained. The phase locking of the buncher with respect to the beam was also set. This bunched beam was fed to the H. E. Sweeper. The H. E. Sweeper could successfully cut down the dark current in between the bunches. The efficiency of the Sweeper was measured to be  $\sim 97\%$ . These results were obtained only in short runs. Unfortunately long runs could not be taken due to the instability in the phase and amplitude in the Sweeper.

### **2.1.9 Upgradation of 6MHz, 500 Watts RF Amplifier for H.E. Sweeper**

The power amplifier driving the High Energy sweeper developed several problems during the test runs. At different power levels low frequency oscillations were picked up by the amplifier resulting in the tripping of the power supply. This problem was solved by using extra capacitive filtering at different points of the amplifier. The gain of the input stage of the amplifier was reduced considerably so that higher RF voltages could be fed in the input. This was done mainly to improve the signal to noise ratio which was required for better timing measurements. The biasing of the MOSFETs were also adjusted and set so as to reduce the third harmonic content in the output to a great extent.

## **2.2 CRYOGENICS**

T.S. Datta, Jacob Chacko, Anup Choudhury, Joby Antony, Manoj Kumar, Suresh Babu, S.A. Krishnan, Soumen Kar, R.S. Meena and A. Roy

In this period, other than the routine operation of cryogenic facility and regular testing of first linac cryostat and cavity in simple test cryostat, a few new systems like re-buncher cryostat, automated helium purifier and the cryogenic data acquisition & control system (CRYO-DACS) have been developed and added to our existing cryofacility. Considering the reduced demand of cryogen, frequency of running the liquid helium plant was comparatively less than the previous two years. Brief report on major activity in the cryogenics group is presented here.

## 2.2.1 Cryostats

### (i) Linac Cryostat :

The first linac cryostat without cavities and superconducting magnet was tested in the previous year for thermal performance with respect to static heat load, cool down time as well as vacuum holding capability, which were satisfactory. Eight cavities have been positioned on support structures, interconnected with pre-cool line as well as with helium vessel. The indigenously developed indium seal Voss clamps to connect the cavities and helium vessel started leaking at 4.5 K with tensile load. To avoid further delay on improvement of existing clamp, the complete coupling assembly has been modified with standard indium seal CF flange. An unsuccessful attempt has been made to cool eight cavities in linac cryostat with the same cooling sequence of buncher. The floating of liquid helium in the helium vessel has been observed with a wide temperature difference (150 K) between cavities and vessel. Same cooling methodology was successful in the case of buncher, where the neck (connection between helium vessel and cavity) diameter was 4 inches against 1.5 inches for linac. It appears that the present neck diameter is less than the critical diameter and liquid flow is blocked by the evaporated gas in the cavity. We are able to cool the cavities in the rebuncher cryostat of similar neck configuration of linac by inserting a quarter inch diameter SS tube to release the evaporated gas from the bottom of cavities.

### (ii) Rebuncher Cryostat :

Rebuncher cryostat is the last cryostat in a series of cryostats for the superconducting linear accelerator. The objective of the cryostat is to rebunch the accelerated beam by using two quarter wave niobium resonators kept at 4.5 K. The height of the cavities in the re-buncher cryostat can be adjusted even when the cryostat is under vacuum by a bellow sealed alignment mechanism. Each cavity can also be aligned with the beam port in x, y, z directions independently. Liquid nitrogen shields are provided in the form of two annular dewars with a floating copper shield inside the dewar to maintain the lower temperature even when the LN<sub>2</sub> level is low. To overcome the difficulty in liquid helium filling, 6 mm diameter SS tubes are inserted in the cavity to release the gas pressure from the cavities.

Another important innovation incorporated in the re-buncher cryostat is the diversion of the cold return helium gas through the pre-cool lines. In other cryostats the cavity and the dewars are pre-cooled by LN<sub>2</sub> prior to the filling of liquid He. By this way the maximum attainable temperature of the dewar and the cavity is only 130K. With the new arrangement, liquid He is transferred into the dewar and cavity when it is at room temperature and the return gas is diverted to the pre-cool lines of the liquid helium dewar and the pre-cool channels of the resonator through a valve. By this method, the temperature can be brought down to 8-10 K and the liquid He filling can be done easily. Total cold

mass of the cryostat is approximately 140 kg, and the diameter is 1.2 meter and the height is 2 meter.

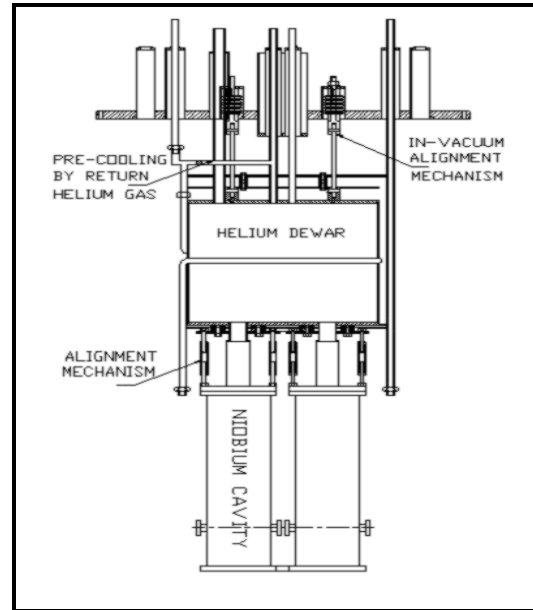


Fig. 12 : Top part of rebuncher cryostat

Fig. 13 : Schematic drawing of rebuncher

**(iii) Simple test cryostat & buncher :**

For regular offline performance testing of cavity, a simple test cryostat with minimum static load was developed in the previous year. In this year the measurement of static heat load at 4.5 K has been repeated with the combinations of cavity and related accessories like RF cable, pickup cable and drive mechanism. The measured heat load is less than 3 W. This cryostat is being used regularly for offline testing of cavity and slow tuner. Liquid helium filling interval was enhanced to 15 - 20 hours against 5 - 6 hours on earlier multipurpose test cryostat. Similarly by inserting copper jacket into the LN<sub>2</sub> shield, filling frequency of LN<sub>2</sub> is only once in a day. Detailed theoretical analysis has been carried out and compared with measured value on shield temperature with liquid level. It is understood that free convective heat transfer co-efficient (5 - 6 W/m<sup>2</sup> K) between unexposed SS surface and copper sheet is very much higher than the conduction heat transfer along the length of shield. It is estimated that top temperature of SS shield with copper jacket is approx. 105 K when level falls below 1 meter against 240 - 247 K without copper jacket. This analysis has been verified by measuring temperature profile on simulation shields.

**2.2.2 Cryogen Distribution line**

Planning and design on extension of liquid nitrogen distribution network to supply cryogen in rebuncher, simple test cryostat and remaining two linac cryostats has been finalized. The vacuum jacketed multilayer insulated transfer line is of similar configuration to the earlier one except the supply valves with valve boxes. Considering the lower range (10 - 40 litres/hr) of flow rate requirement, valves with lower C<sub>v</sub> is preferred. Simil-

arly the design for liquid helium supply and return gas connection between valve box-4 and rebuncher cryostat has been finalized. Fabrication will be initiated shortly.

### **2.2.3 Helium purifier & gas analysis setup**

An automated external helium purifier has been designed and developed indigenously at NSC and integrated with helium recovery system. The purifier works on the principle of adsorption by charcoal at 78 K. Before the installation it has undergone various testing regarding its vacuum holding capability in room temperature as well as at liquid nitrogen temperature. During commissioning a leak was detected at the filling port of charcoal bottle. The leak enhances when the system cools down at 78 K and adsorber bed is pressurized to 15 bar. A turbo pump of capacity 250 lps was assembled directly on top flange and achieved vacuum is in the order of  $10^{-6}$  torr at operating condition. The static evaporation rate of liquid nitrogen is reduced from 2 litres/hr to 1 litres/hr by wrapping 4 layers of MLI on the annular vessel. The dynamic liquid nitrogen consumption is 5 litres/hr with an impure gas flow rate of 45 NM<sup>3</sup>/hr. This agreed well with the calculated design value. Low consumption of liquid nitrogen is possible by using the heat exchanger for exchanging cold enthalpy of return pure helium gas. Without this the LN<sub>2</sub> consumption could have been 30 litres/hr for the same purification capacity. The purifier has been operated with various inlet impurities up to a maximum of 10% air impurity and breakthrough capacity has been obtained. For an air impurity level of 1%, the purification capacity is 180 NM<sup>3</sup> with a purity better than 99.999%. Locally developed capacitance type liquid nitrogen level indicator along with the meter is integrated here for automatic filling of cryogen.



**Fig. 14 : Helium purifier**



**Fig. 15 : MLI setup**

An indigenously developed gas analysis set up with multiway valve to trap gas from different locations and a manifold of calibration gases is being used regularly while running the purifier as well as liquefier. At present the gas analysis set up consists of an arc cell to measure nitrogen impurity (less than 100 PPM) in helium, a thermal conductivity detector to have information on total air impurity in helium, a dew point monitor and one oxygen analyzer. An analyzer to measure oil mist in helium has been procured and it will be integrated with gas analysis set up after calibration.

#### **2.2.4 Experiments on MLI set up**

A calorimeter of stainless steel (SS) with guarded vessel has been developed to study the performance of different sets of multilayer insulation (MLI) and aluminium tape on SS pipe at 4.5 K. On our first attempt to measure the radiation load at 4.5 K on bare surface of mechanically polished SS surface, heat load higher than calculated value is observed. To find out the source of additional heat load, experiment with various combination of temperature (300 K - 80 K, and 80 K - 4 K) have been carried out. From these experiments it is confirmed that the effective emissivity of SS is matching with literature value and the surface is without oil or grease. When both shield as well as experimental vessels are at liquid nitrogen temperature, conduction through SS pipe is the dominant heat transfer mechanism and measured value appears to be higher. The conduction

heat transfer through the leads of temperature sensors and Joule heating is removed by isolating from top connector. On our last attempt, it is observed that angular radiation from top plate to the curved surface of experiment vessel is contributing a good percentage of unaccountable heat transfer. Some more experiments will be conducted with liquid helium to evaluate the contribution of different modes of heat transfer. The insulation will be wrapped on experiment vessel after finding out the reason of hidden heat transfer on bare surface.

### **2.2.5 Cryogenic facility**

#### **(i) Helium plant :**

The plant was operated 8 times, mostly in open loop mode to meet the demand of liquid helium on carrying out the test on STC and MLI. The total estimated production was 25,000 litres which is less than in previous year. Remote control operation of compressor from the cryogenics control room is very much useful and convenient on loading, unloading, emergency start in the event of power failure. Repair of pneumatic controller for LN<sub>2</sub> supply and pure gas supply valve have been carried out successfully. Cool down time of helium refrigerator has been reduced from 14 hours to 8 hours on starting the warm expansion engine along with compressor.

#### **(ii) Liquid Nitrogen Plant :**

The plant was operated 2132 hours and estimated liquid nitrogen production was 1,06,660 liters to meet the demand on running helium liquefier and precooling of cryostats. In addition 95,000 liters liquid was procured for other users in NSC.

#### **(iii) Helium purification :**

Based on recovery compressor running hours, it is estimated that impure helium gas of 2000 NM<sup>3</sup> has been purified in this period.

### **2.2.6 Miscellaneous work**

A basic experiment has been conducted to have the information on influence of thermal contact for Lakeshore sensor reading. It is concluded that thermal anchoring of leads plays dominant role rather than the contact of sensor body with SS.

The kit to convert manually operated liquid helium valves to a proportional valve controller was assembled and tested externally. Similarly an adapter has been designed and developed to convert manual regulating valves into pneumatically controlled on-off valves with a compact size. MS platform in the beam hall-2 has been extended to suit the control and power cable tray installation.

## 2.2.7 A VME based Cryogenic Data Acquisition & Control System

Joby Antony & Raj Kumar

The NSC cryogenic network is computer controlled using a newly developed Data Acquisition & Control System named "CRYO-DACS". A large number of analog and digital cryogenic related data from five beam-line Cryostats, two helium com-

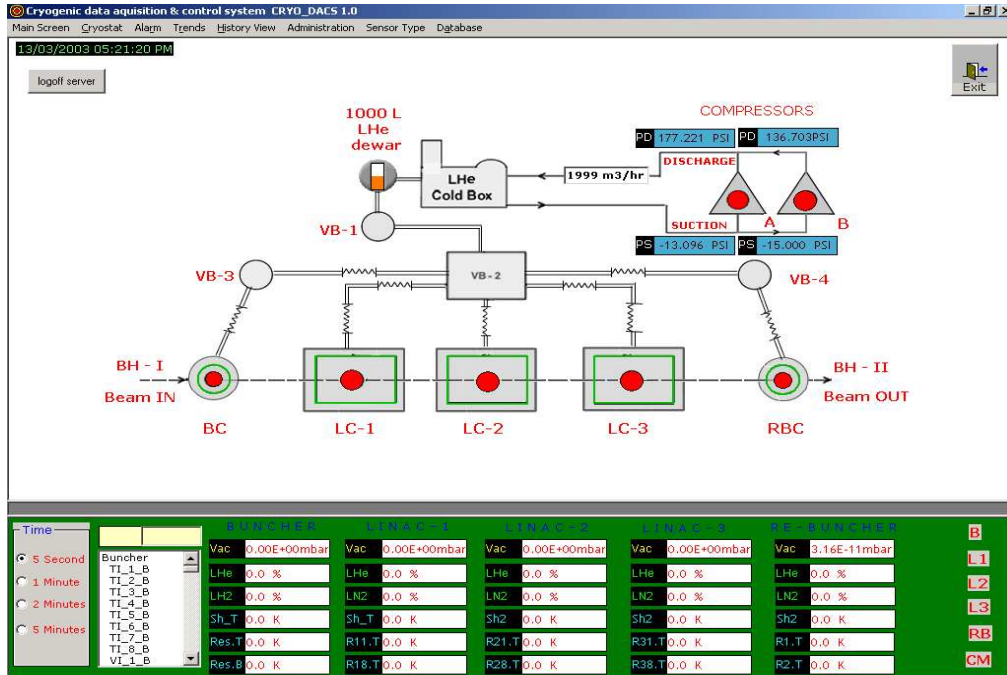


Fig. 16a : The main screen of Cryo-DACS

pressors, liquefier, cryogenic distribution lines etc. are brought from different locations to a central cryogenic control room for remote control, monitoring and analysis. The main cryogenic parameters measured and monitored are temperature, pressure, vacuum and cryogenic fluid levels across a network and the system performs closed loop controls of cryogen valves with individually programmable LLT & ULT settings on-line. The system is operational.

### i) System details

#### a) Hardware

The hardware architecture of CRYO-DACS is single-host multi-crate distributed VME bus with embedded VxWorks, all linked by workstation clients in 100 Mb/s LAN for distributed logging, historical trending, analysis, alarm management and control GUIs. The system is presently installed with two VME crates (6U) distributed far apart at two distant locations approximately 90 meters apart. The crates and modules are procured from M/s VME Microsystems International Corporation, USA. The modules used

are analog inputs, digital inputs and outputs. The AI modules used are VMIVME 3113-A & 3801 both 12 bit differential ADCs and VMIVME 2536 for digital input-outputs. The CPU used is VMIVME 7698 with embedded RTOS VxWorks. Two HP servers have been installed at the central cryogenic control room to act as development host and operator consoles.

## **b) Electronics**

The various controllers required for the project eg. thermometry electronics required for the low temperature measurements and vacuum interlock controllers are designed and developed indigenously. The other controllers used for LN<sub>2</sub> & liquid He level measurements are procured from LAKESHORE.

## **ii) I/O Parameters**

The total number of I/O presently involved with the project are 314, expandable in future. The main analog parameters measured and acquired are cryostat temperatures [4.2 to 350 K], LN<sub>2</sub> pressures [0-4 bar], liquid He pressures [-1 to +1 bar] , vacuum [ $10^{-9}$  mbar- atm], LN<sub>2</sub> levels[ 0-100 %] and liquid He levels [0-100%] whereas the digital inputs are for status readbacks from valves and vacuum systems. The main helium compressor parameters acquired are suction (-15 to +15 psi) & discharge pressures (-15 to +300 psi), oil temperatures (0-120 deg. C), power (0-300 kW), loading (0-15 turns), unloading (0-15 turns) etc. and a large number of control outputs for loading, unloading, start, stop, reset etc.

## **iii) Software**

The software development is done in two parts. The first part i.e. IOWORKS MANAGER, a development center and a cross-tool, has been used to configure an NT based host which acts as a development system for VxWorks based targets . The tool VISUAL IOWORKS has been used for the development of real-time VME bus access, which supports a group of class libraries for VxWorks operating system. The application developed is downloaded and run on VxWorks targets from the host . The six C++ logic modules, each specific to any one application namely buncher, linac1, linac2, linac3, re-buncher, compressor are hot-swapped into the target online. The second part, a graphics package for OPC client & supervisory control and data acquisition, has been developed using VISUAL BASIC for the real time data fetching, logging, trends, analysis and control GUIs. This package can be run from any client in the cryogenic as well as NSC LAN for remote operations. The OPC (OLE for process control) server-client communication method is used to collect data from remote VME targets and record into an RDBMS backend (ACCESS-2000) and further retrieved using ADO for graphical analysis. The distributed multiple logging allows multiple users to log data simultaneously in different

sampling intervals from 1 sec and above. Powerful tools have been developed for the graphical comparison of analog & digital data on-line or off-line.

The control GUIs to control valves in automatic and manual modes, remote controls of compressors etc. are done from control room consoles or can be done from any other client. Closed loop controls of LN<sub>2</sub>, liquid He valves have been tested successfully for auto refilling. The entire closed loop controls will not be affected even if the host computers in control room goes off as target program stays embedded. The LLT and ULT settings of closed loop controls can be dynamically programmable online.

#### **iv) Networking**

A separate 100 MB/s local cryogenic network has been laid to isolate the cryogenic traffic from main LAN. A Windows-2000 server has been configured at the control room to act as a host and a gateway. This gateway separates local-cryogenic LAN (192.1.3.XX) from main NSC-LAN (192.0.3.XX) and it uses route and remote access service (RRAS). Another server running WIN-2000 is configured as a backup domain controller to the above primary domain controller in CRYODACS-DOMAIN. Both servers run terminal services. Any user who wants to run experiment near to any cryostat can simply hookup his client LAPTOP/PC running WINDOWS or LINUX to the TCP/IP port provided near to each cryostat and start logging and analyze data locally.

#### **v) Signal conditioning**

Output signals from most transducers required conditioning in order to adjust the signal level to be compatible with the assigned 12 bit ADCs in the range of 0-10 V dc. The current signals in the form of 4-20 mA and 0-20 mA are converted to multiple isolated 0 -10 V dc using MTL make signal conditioners. Such 20 signal conditioners are installed. All analog signals are filtered at 50 Hz prior to feeding into ADCs internally. A separate clean earth has been laid only for CRYO-DACS to separate all electrical noises in the system.

The cabling of approximately 2000 terminations is done using individual and overall shielded multicore instrumentation cables only. Conditioning of thermometry signals from each cryostat (totalling 100) is done to 0-10 volts standard in the local racks using controllers built in house. All the VME digital input, outputs are optically isolated 24-28 volt standard. The cabling of additional 94 signals required to be given to the main CAMAC based control room in the form of 0-10 V dc, 24 V D/I etc are also terminated in the central rack. Two UPS systems of 2 KVA capacity have been installed to power all local racks, central rack, VME crates, valves, control room and all devices of CRYO-DACS to ensure round the clock operations.



**Fig. 16b : The Central Rack**

## **2.3 RF ELECTRONICS**

B.K. Sahu , Ashutosh Pandey , S. Venkataramanan and B.P. Ajithkumar

### **2.3.1 Status of 97 MHz Power Amplifier for LINAC**

Since the dynamic phase control mechanism is being adopted for Linac superconducting resonator control, considerable increase in requirement of power from 200 watts to 400 watts power is expected. A power amplifier capable of delivering 400 watts (CW) at 97 MHz has been successfully developed. This amplifier is built with a circulator and dummy RF load. A working prototype has been given to M/s. BEL, Bangalore for production.

Meanwhile, at RF laboratory we have improved upon the existing power amplifier design of 250 watts. The features included are (i) Circulator with RF dummy load (ii) Remote "ON/OFF" control (iii) Remote "STATUS" readback and (iv) Compact SMPS.

### **2.3.2 Status of Resonator Controller Modules**

Since the dynamic phase control mechanism is being well tested with NSC linac superconducting resonators the production work for the same is being carried out at Electronics Division, BARC, Mumbai. All the RF electronics module required for the First Linac cryostat has been produced locally using support electronics module. The Modules are housed in two specially designed NIM bin to control eight resonators. Each NIM bin will house the following modules (i) Four Resonator control Module (ii) One Reference Module (iii) One Input Module and (iv) One Multiplexer Module. The router will be designed to take care of the CAMAC control of the Modules for remote operation.

## **2.4 BEAM TRANSPORT**

A. Mandal, Rajesh Kumar and S. Suman

The task of this group is to develop the Beam Transport System for LINAC beam lines. Projects have been undertaken for indigenous development of different magnetic elements and control electronics needed for LINAC beam lines. Status and development during the last year are described below.

### **2.4.1 Quadrupole Magnets**

A. Mandal and S. Suman

Five quadrupole triplet magnets were fabricated for LINAC beam lines. These magnets have been tested. Testing includes the following:

Checking insulation between yoke and coils.

Checking of water connection.

Checking polarity of three quadrupoles.

Study of excitation to determine maximum field gradient.

Checking magnetic centre.

Measurement of temperature rise

### **2.4.2 High Field steerers**

S.K. Saini and A. Mandal

This year four more steerers have been fabricated in our workshop. Fabrication of heat sinks and other activities for these magnets are in progress.

### **2.4.3 IGOR modules**

Rajesh Kumar, S. Suman and A. Mandal

This single width CAMAC based module is used to control the magnet power supply through CAMAC in remote operation. 20 numbers of such modules have been fabricated in house and tested. Many are in use in Pelletron. The indigenous frame used gives some mechanical problem in fitting in new CAMAC crates procured. The PCB was remounted to fit properly in this crate. This year we are planning to fabricate 10 more IGOR modules. These will be mounted on the imported module procured from Kinetic Systems, USA.

### **2.4.4 Switch gear for magnets in LINAC beam line**

Rajesh Kumar, S. Suman, Raj Kumar and A. Mandal

In LINAC there are one Quadrupole triplet and two steerers in each beam line. Since beam is switched to one beam line at a time, these magnets at different lines are energized from a single set of power supplies. This needs a switch gear system to select the magnets from one beam line to another. This consists of seven motor gears for seven beam lines, which are controlled by a remote controller. A complete system has been designed. Control electronics have been developed and tested. The motors were imported from Danfysik and have been assembled in two cabinets. All the motors and control modules have been assembled in two cabinets. The complete system has been assembled and the performance has been tested. The system is working fine.

### **2.4.5 Switch Mode Power Supply for Superconducting Solenoid magnets**

Rajesh Kumar, S. Suman and A. Mandal

A 10V/100A power supply has been developed using switch mode technique to power super conducting magnet. It is a constant current and constant voltage power supply with an automatic crossover feature. After thorough testing of the prototype module, five power supplies have been fabricated by local vendors. These power supplies have been tested.

### **2.4.6 Super Conducting Magnet Power Supply Programmer**

Rajesh Kumar, S. Suman and A. Mandal

The power supply programmer is an integral part of the super conducting magnet system. When the magnet power supply is used manually to increase or decrease the current, the high inductance of the magnet may interact with the power supply and cause the current to oscillate. The power supply programmer ensures smooth charge and discharge

of magnet current, which eliminates oscillation and stabilizes the super conducting magnet system. The programmer has been designed and assembled in house and tested successfully at NPL with super conducting magnet. The design is final for mass production. Five such programmers have been fabricated.

#### **2.4.7 Persistent Switch Heater Power Supply**

Rajesh Kumar

The Persistent switch heater power supply has been developed and fabricated to heat a persistent switch mounted across the super conducting magnet, into the resistive state. A key operated switch is provided to enable the output to reduce the possibility of accidental persistent switch activation. The output is adjustable from 0 to 100 mA by means of a rear panel mount potentiometer. The design is final and ready for mass production.

#### **High Current High Stability Magnet Power supply (200A/50V, 5PPM/8 hrs)**

Rajesh Kumar, T. Varughese, A. Jhingan, S. Suman and A. Mandal

A project has been undertaken to prove the feasibility of development of high stability high current power supplies which can be used for quadrupole, dipole and bending magnets. It is linear DC current regulated power supply based on series pass linear technology. Functional and performance test has been carried out using HIRA quadrupole magnet as a load. The stability achieved was 2PPM/8hrs.

#### **2.4.9 Faraday Cup Controller**

S. Suman, Rajesh Kumar and A. Mandal

Ten Faraday cup controllers are being fabricated for Phase-II. This controller can operate Faraday cup through Remote as well as Local for Cup IN/OUT. It provides 24V/110V for energizing solenoid of Faraday cup. It also provides the - 400VDC to suppressor of Faraday cup. 10 Faraday Cup Controllers have been fabricated this year and these have been tested.

#### **2.4.10 Spark Protection Modules**

S. Suman and A. Mandal

The spark protection modules are used to suppress the spikes from data lines to different CAMAC modules. 30 Spark protection modules for LINAC beam lines have been fabricated and tested.

#### **2.4.11 SMPS Controller**

S. Suman, Rajesh Kumar, Kundan Singh and A. Mandal

A project has been taken to develop 5 nos. of SMPS controller for operation of super conducting magnet power supply through CAMAC. The module basically sets the current (0-100A) to SMPS programmer, reads the magnet current (0-100A) and also displays the status of magnet and power supply. A prototype has been developed and tested. 5 nos. of such modules are to be fabricated this year.

#### **2.4.12 PSTV Controllers**

P. Barua and A. Mandal

A project has been undertaken for fabrication of PSTV controllers. The design is complete and the different components have been procured. Order for fabrication is to be placed.

#### **2.4.13 Extension of Zero degree Beam line**

P. Barua, A. Kothari and A. Mandal

Beam line from first cryostat to Switching Magnet is being extended. As the second and third cryostat are not being installed at present, the original design is modified and one extra quadrupole triplet is placed instead of cryostats for proper focussing of beam. The magnets have been aligned and the installation of the rest of the equipments is going on. All the racks have been placed in proper places. Cable trays have been laid down for running cables from control room to different instruments in beam hall.

#### **2.4.14 Development of 43 kVA H-class Air Cooled Linear Voltage Regulator & six phase Double Delta Transformer for 300 A, 100 V DC Power Supply**

Raj Kumar and Rajesh Kumar

The above linear voltage regulator has been developed in vertical column type construction where rolling contacts collect the current while correcting the voltage. This has super enameled copper strips of size 13x4 mm. The winding is edge type without any paper insulation. The balancers are used in between the two sets of current collecting rollers as the current is being collected from two opposite sides of the winding turn. A synchronous motor of 20 Kg-m torque moves the rollers through the guides. The regulator is having H class insulation and is completely air cooled.

The six phase step down transformer is having star connected input winding and delta connected double output winding. The output delta windings has been formed by connecting the two windings of different limbs in series forming one winding and then connecting them as delta to have 60 degree phase difference between the ends. This transformer is also wound using the 13x4 mm super enamelled copper strips. Proper cooling ducts have been created between the windings to have it air cooled.

### **2.5 LOW ENERGY ION BEAM FACILITY (LEIBF)**

G. Rodrigues, P. Kumar, U.K. Rao, C.P. Safvan,. D. Kanjilal and A. Roy

The facility has been used for various experiments and source related development work all through the year except for some period for maintenance and improvement of transmission through the 90° beam line. The source has been performing satisfactorily with mostly gaseous type of ions and for a few runs using the MIVOC (Metal Ions using Volatile Compounds) technique for developing silicon beam. Due to demand from the user community for silicon beam, we thought of various possibilities of producing silicon beam in terms of reasonable currents without using toxic gases. The only possible solution was to use the MIVOC technique where one uses a compound which has a vapor pressure of the order of  $10^{-3}$  mbar at room temperature. Therefore, one of the gas bottles was replaced with a small MIVOC chamber containing trimethylchlorosilane in order to produce this beam. Initial results have been found to be encouraging. In future, we plan to install the MIVOC chamber at source potential in order to improve the conductance and to be able to remotely control the opening of the chamber valve for proper optimization. For cases of argon and nitrogen, when helium was used as the mixing gas, the enhancement factor was found to be 6.3 for  $\text{Ar}^{6+}$ , 23.5 for  $\text{Ar}^{7+}$ , 2.4 for  $\text{N}^{4+}$  and 4.8 for  $\text{N}^{5+}$ . For oxygen, without using

mixing gas, the beam currents obtained were as follows; 350  $\mu\text{A}$  for  $\text{O}^{1+}$ , 300  $\mu\text{A}$  for  $\text{O}^{2+}$ , 180  $\mu\text{A}$  for  $\text{O}^{3+}$ , 11  $\mu\text{A}$  for  $\text{O}^{5+}$ , 5  $\mu\text{A}$  for  $\text{O}^{6+}$  and 130 nA for  $\text{O}^{7+}$ .

In one particular experiment, we measured the outputs of each individual charge state of oxygen by varying the extraction voltage from 6 kV up to a maximum of 18 kV and by keeping the total  $E/q = 75$  keV. All other parameters like gas flow, rf power and rf tuning stub were frozen except the einzel lens. The extraction pressure was maintained at  $3.7 \times 10^{-7}$  torr with a total rf power of 1 W. It was observed (Fig. 17) that the maximum outputs for each increasing individual charge state approximately peaked at corresponding lower extraction voltages (charge states corresponding to 5+, 6+ and 7+ are not shown due to space constraints). For a narrow acceptance of a system which is presently considered in our case, this behavior roughly follows the formula for the transverse emittance of cold ions from the source which is proportional to  $q^{3/2} V^{-1/2}$  where  $q$  is the charge state of interest and  $V$  is the extraction voltage.

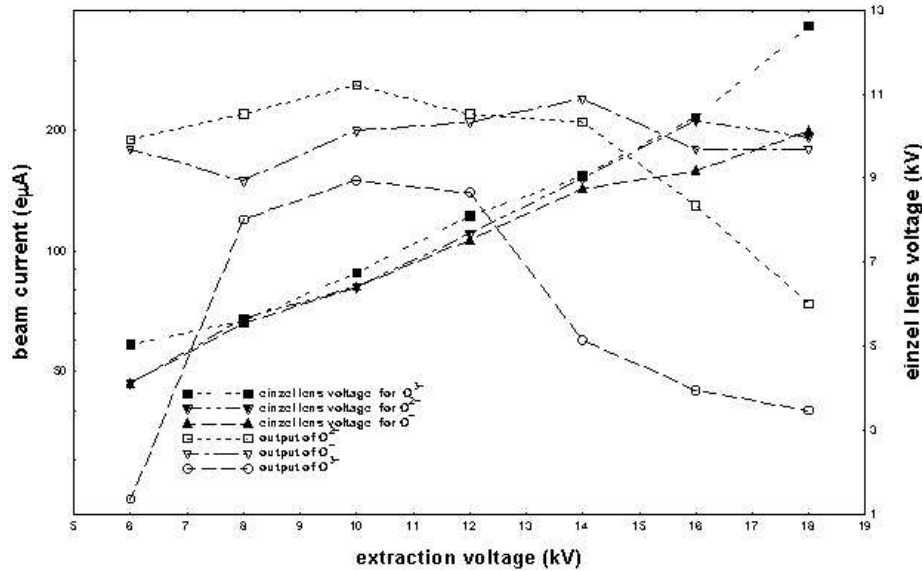


**Fig. 17 : Beam currents of  $\text{O}^+$ ,  $\text{O}^{2+}$  and  $\text{O}^{3+}$  as a function of extraction voltage**

Due to severe losses in beam transmission through the  $90^\circ$  beam line, it was felt that the electrostatic quadrupole triplet be brought closer to the image plane corresponding to the analyzing magnet and aligned accurately so that the losses in beam intensity be minimized. The  $90^\circ$  line consisting of other components like faraday cup, double slit, beam profile monitor, electrostatic scanner, experimental chamber and new components like electrostatic steerers were re-aligned properly and this resulted in improved transmission to the experimental areas (Fig. 18). The old accelerating tube which had a smaller acceptance and associated problems has been replaced with a new one having relatively larger acceptance.

A facility for off-line electrical measurements at low temperatures (near to 10 K) has been installed. Resistivity measurements of a composite material consisting of La, Ni and Fe at 10 K were carried out and it was found that the measured values were orders of magnitude different from that at room temperature. A general purpose 4 kV, 4 mA variable power supply (both positive and negative) has been designed and developed for use in beam lines.

**Fig. 18 : 90° beam line after modification and re-alignment**

Experimental activities were also initiated towards understanding the processes taking place within the plasma in the ECR source. Diagnostics in the form of X-ray and optical spectrometers were set up and the feasibility of undertaking atomic and molecular physics experiments utilizing the ECR plasma were demonstrated. For X-ray spectrometry, the flange at the back end of the ECR source was modified by inserting a Mylar window. The X-ray detector (Amptek) was installed outside the high voltage deck. X-rays produced in the ECR source were measured by this detector, while varying the source parameters. The X-rays from the ECR source (Fig.

19) consist both of characteristic lines that depend on the plasma constituents and bremsstrahlung radiation that changes with the electron temperature. The study of the bremsstrahlung radiation as a function of the source parameters therefore provides us a handle on the efficiency of the hot electron production which is responsible for the production of highly charged ions in the ECR source. Similarly, an optical spectrometer has been set up along the extraction axis of the ECR source. A SPEX spectrometer (range 350-500nm) has been installed and optical spectra can be measured as a function of the source parameters. The idea is to study the evolution of excited states within the plasma by looking at the optical emission from such atoms.

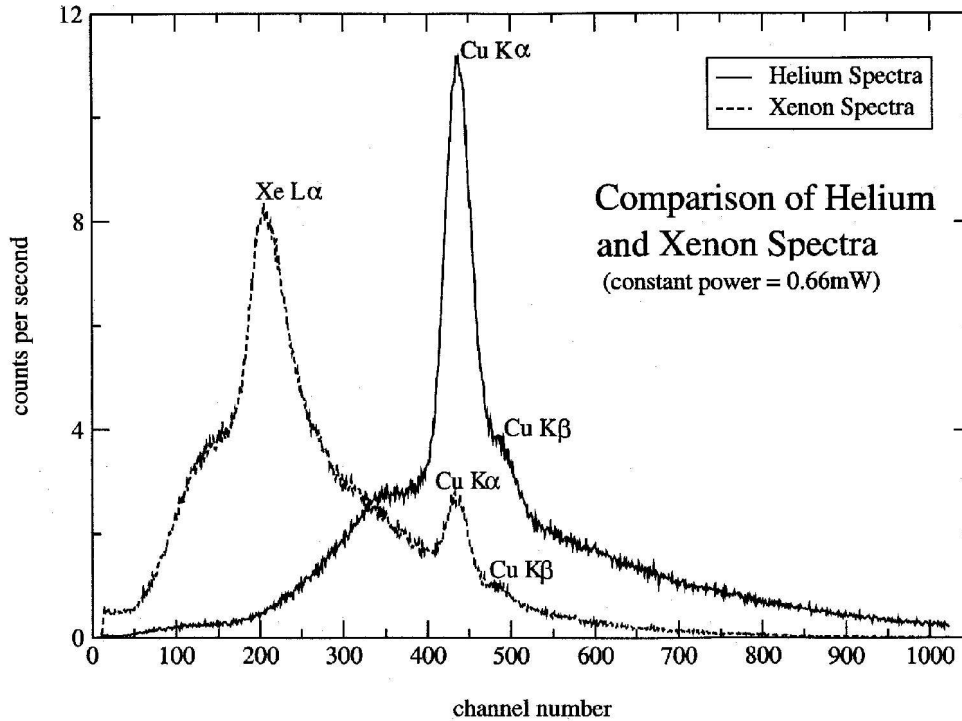


Fig. 19 : X-rays from the ECR source

Table 1 : List of experiments performed in the Low Energy Ion Beam Facility

Experiment	Beam	Dose (particles/cm <sup>2</sup> )	Energy
Silicon implantation on quartz	Si <sup>3+</sup>	1.0 x 10 <sup>15</sup> , 2.5 x 10 <sup>15</sup> , 5.0 x 10 <sup>15</sup> , 7.5 x 10 <sup>15</sup> , 1.0 x 10 <sup>16</sup> , 2.5 x 10 <sup>16</sup>	225 keV
Formation of SiC and ion beam annealing by argon	C <sup>2+</sup> , Ar <sup>2+</sup> , Ar <sup>4+</sup>	1.0 x 10 <sup>16</sup>	150 keV, 300 keV
To study the electrical properties of Si after ion implantation	Ar <sup>2+</sup>	5.0 x 10 <sup>13</sup> , 5.0 x 10 <sup>14</sup> , 5.0 x 10 <sup>15</sup>	150 keV

Experiment	Beam	Dose (particles/cm <sup>2</sup> )	Energy
Phase formation of SiC at high temperatures	C <sup>2+</sup>	2.0 x 10 <sup>17</sup>	200 keV
Production of oxygen vacancies in ZnO nanocrystals embedded in SiO <sub>2</sub> matrix	Ar <sup>4+</sup>	1.0 X 10 <sup>15</sup> , 1.0 x 10 <sup>16</sup> , 1.0 x 10 <sup>17</sup>	500 keV

## 2.6 HIGH CURRENT INJECTOR

### 2.6.1 Design of a High Temperature Superconducting Electron Cyclotron Resonance Ion Source for the High Current Injector of LINAC

D. Kanjilal, G. O. Rodrigues, C. Bieth<sup>1</sup>, S. Kantas<sup>1</sup>, P. Sortais<sup>2</sup>, C. P. Safvan, P. Kumar, U. K. Rao, A. Mandal and A. Roy

<sup>1</sup>Pantechnik, rue Alfred Kastler, 14000 CAEN, France

<sup>2</sup>Institut des Sciences Nuclaire, INS-IN2P3, Grenoble, France

#### (i) *Introduction*

A new type of high temperature superconducting electron cyclotron resonance ion source (HTS-ECRIS) to be operational at 14 to 18 GHz on a 350 kilo volt (kV) platform with minimum requirements of electrical power and cooling water on the platform has been designed as a collaborative developmental project between Nuclear Science Centre (NSC, New Delhi), Pantechnik (Caen), and Institut des Sciences Nuclaire (INS-IN2P3, Grenoble). The HTS-ECRIS will provide high current multiply charged positive ion beams for injection into the superconducting linear accelerator (SC-LINAC) after pre-accelerating the beams to matching energy using radio frequency quadrupoles and low velocity superconducting resonators.

#### (ii) *Design features*

In the present design the HTS coils will be used in designing the high performance positive ion source PKDELIS for the required mass to charge ratio (A/q) of ~7 for high current injector (HCI) of NSC. Since no cryogen can be transferred across the high potential of 350 kV, a new type of high temperature superconducting (HTS) coils of Bi-2223 were chosen to reduce the power and cooling requirements for producing the large axial magnetic fields required for running the ECRIS at UHF frequencies up to 18 GHz. These HTS coils will be operated in a superconducting mode at a temperature of about 30 K by using cryo-coolers (Gifford-McMahon type) placed on the high voltage (HV) platform itself. The electrical power required

to produce the high magnetic field will be about 10 kW. The power needed for operation of the HTS-ECR on the 350 kV platform will be limited to  $\sim 50$  kW. Cooling requirements on the platform will also be drastically reduced compared to the existing copper coil based ECRIS and will be met by using mainly air-cooling and standard closed loop cooling system mounted directly on the platform. The calculation of the axial field profile by the POISSON group of codes [1] using solenoid coils made of BSSCO-2223 HTS wires at an operational current density of  $90 \text{ A mm}^{-2}$  has been done. The hexapole design is based on the design of the Halbach [2] configuration and is made of permanent magnets comprising of Nd, Fe, and B. Surface treated magnets will be used for high temperature and high humidity applications. The 3D calculations of hexapole fields using minimum possible values of  $B_r$  have been done for both 24 sectors and 36 sectors. The resultant ECR surface arising from the superposition of the axial and radial fields has been calculated by the TRAP-CAD code [3]. At the designed frequency of 18 GHz, the length, diameter, volume and surface area of the ECR surface was found to be 31 mm, 29 mm,  $11.8 \text{ cm}^3$  and  $26 \text{ cm}^2$  respectively. The ion optical calculations of the extraction system in the presence of the strong axial field produced by the HTS coils has been worked out using the IGUN code [4]. For example, trajectories of oxygen beams in various charge states, for an extraction voltage of 35 kV (bias voltage of the plasma tube) and puller voltage of -20 kV for total source current of 10 mA inside the puller has been calculated.

(iii) *The source configuration*

The source configuration is based on the HYPERNANOGAN ECR ion source. The plasma chamber will be made of high purity aluminum so that the oxide formation on the aluminum surface will enhance the secondary electron emission properties of the source. For the iron yoke, high quality materials have been chosen in order to achieve relatively high fields. The cryostat to house the coils will be manufactured entirely from 300 series stainless steel and is in two main sections. A very useful design feature is that access can be gained to the cryo-cooler without having to dismantle the iron yoke that the coils sit within. Each coil is made up of 10 pancake layers wound as double pancakes and separated by epoxy-glass 10G40 insulation. The coils will be wound onto a high conductivity copper former for support and to provide a path for heat to be conducted away from the coils to the cold head of the cryo-cooler.

(iv) *Design of Injector Magnet*

A  $90^\circ$  injector magnet has been designed to select the particular ion and to eliminate unwanted ion species produced in ECR source. This reduces the current loading of the high voltage power supply used to pre-accelerate the ions from ECR. The magnet has been designed for the following beam parameters:  $M/q = 10$ , emit-

tance =  $200 \pi$  mm. mrad,  $ME/q^2 = 0.3$  amu MeV, Magnet rigidity ( $B\rho$ ) = 0.08 T m. The design aim is to have minimum weight, good acceptance, reasonable mass resolution and no water cooling. To minimize weight, the radius of the magnet is taken to be 0.3 m and  $B_{\max} = 0.3$  T. The gap of the magnet is taken to be 80 mm to match the large emittance of the beam. For point to point double focussing the mass resolution is  $1.7 \times 10^{-2}$  for a slit size of 10 mm. The beam optics has been calculated for point to point double focussing using the TRANSPORT [5] program. By including gap effect, the entrance and exit angles turn out to be  $31.6^\circ$  for double focussing. To minimize spherical aberrations we have incorporated curvatures in the entrance and exit edges and sextupole components. The detail design is in progress.

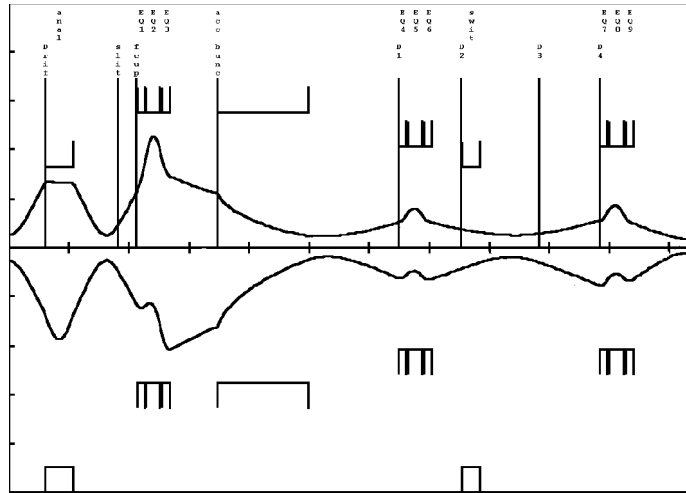


**Fig. 20 : Beam envelope from ECR source up to RFQ entrance**

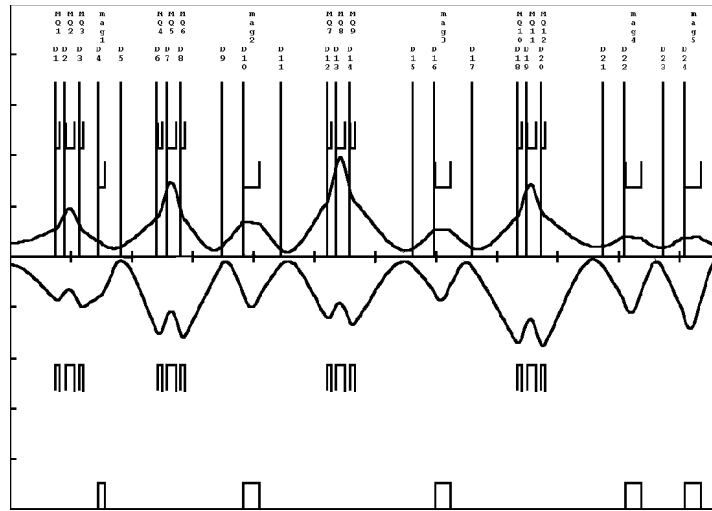


**Fig. 21 : Beam envelope after RFQ, upto entrance in beam hall 1**

## REFERENCES

- POISSON/SUPERFISH group of codes, Los Alamos National Laboratory, Los Alamos  
K. Halbach, Nuclear Instruments and Methods, **169**, 1 (1980)  
J.Vamosi and S.Biri, Comp. Phys. Comm., **98**(1996)215, [www.atomki.hu/atomki/ECR/trapcad.htm](http://www.atomki.hu/atomki/ECR/trapcad.htm)  
R. Becker, Rev. Sci. Instrum., **63** (4), 2756 (1992)  
TRANSPORT, PC Version, Urs Rohrer, PSI, Switzerland